Geogr. Fis. Dinam. Quat.
38 (2015), 55-66, 8 figg., 6 tab.

DOI 10.4461/GFDQ.2015.38.06

GERALDINE QUÉNÉHERVÉ (*), FELIX BACHOFER (**) & MICHAEL MAERKER (*,**)

EXPERIMENTAL ASSESSMENT OF RUNOFF GENERATION PROCESSES ON HILLSLOPE SCALE IN A SEMIARID REGION IN NORTHERN TANZANIA

ABSTRACT - QUÉNÉHERVÉ G., BACHOFER F., & MAERKER M., *Experimental Assessment of Runoff Generation Processes on Hillslope Scale in a Semiarid Region in Northern Tanzania.* (IT ISSN 0391-9838, 2015).

In runoff modelling often saturated conductivities or infiltration rates for saturated surfaces are used to calculate the soil water balance and subsequently surface runoff. These infiltration rates are often too high and thus no or very little runoff is generated. However, after long dry periods even with small precipitation events surface runoff is observed. In this study we focus on the infiltration rates at different tensions to study their effect on surface runoff generation on a typical soil catena of northern Tanzania. The area is characterized by very little information on surface runoff and soil characteristics. Therefore, we measured soil infiltration and texture at the surface as well as overland flow volumes for individual rainfall events between October 10, 2010 and December 6, 2010 using a simple experimental setting. We examined rough water balance quantities for single rainfall events. A simplistic hydrological modelling of the surface runoff and accumulation was performed and compared to measured surface runoff. The study shows that infiltration at 0 water tension clearly overestimates infiltration quantities. However, even when soil characteristics like crusting of sealing are not considered, our simple approach yield much better surface runoff volumes using infiltration rates at higher soil water tensions instead of saturated infiltration conditions. The interaction between rainfall and soil surface conditions is relevant for understanding the hydrology of semiarid savannas with gentle slopes. However, we show that our approach integrating simple field measurements and basic hydrological budget models yield much better results than conventional approaches.

KEY WORDS: Surface Runoff; Hydrological Modelling; Rainfall-Runoff; Hillslope Scale; Tanzania; Surface Runoff Detectors.

INTRODUCTION

Runoff generation in direct response to a precipitation event triggers soil particle detachment and accordingly soil erosion phenomena which are a major threat in sparsely vegetated regions. The factors affecting runoff for event-based analyses are i) rainfall characteristics and climatic conditions (rainfall intensity, duration and distribution), ii) the soil type (soil evaporation, infiltrability, hydraulic conductivity, antecedent condition of the soil moisture, water repellent characteristics, bulk density, surface crusting and surface roughness), iii) vegetation (vegetation cover, organic matter, macropores and root systems), and iv) the catchment area (slope steepness, slope length, landscape position) (after Critchley & Siegert, 1991; Borselli & *alii*, 2001; Bracken & Croke, 2007; Ritter & *alii*, 2011).

However, for a detailed surface runoff assessment especially the soil parameters are often not available or only hardly obtainable requiring sophisticated instruments, trained personnel and the economic resources to measure them. Particularly, semiarid areas around the globe are often characterized by scarce infrastructure and rural environments with no or sparse information on the spatial distribution of soils or related parameters on institutional levels. Moreover, semiarid regions generally show low precipitation that is highly variable (Sala & Lauenroth, 1982; Mualem & Assouline, 1996). Hence, simple low budget approaches are needed to overcome these problems.

In order to assess surface runoff processes in semiarid areas, precipitation events have to be addressed as pulses,

(*) *Institute of Geography, University of Tübingen, Ruemelinstr. 19-23, 72070 Tuebingen, Germany.*

(**) *Heidelberg Academy of Sciences and Humanities, c/o University of Tübingen, Ruemelinstr. 23, 72070 Tübingen, Germany.*

(***) *Dipartimento di Scienze della Terra, Università di Firenze, Italia.*

Corresponding author: Geraldine Quénéhervé, Tel.: +49 7071 2972131. E-Mail address: geraldine.queneherve@uni-tuebingen.de

This work was funded by the Heidelberg Academy of Sciences and Humanities' research centre: 'The Role of Culture in Early Expansions of Humans'. We thank the Tanzania Commission for Science and Technology (COSTECH) for their support and the Manyara Ranch Conservancy, held in trust by the African Wildlife Foundation (AWF) up to 2013, for their access permit. Furthermore, we would like to thank Hauke Sattler for the assemblage of the surface runoff detectors. Finally we would like to thank the EU IRSRS project FLUMEN for support and assistance.

Fig. 1 - Surface runoff shortly after a precipitation event of 15 mm (in 40 min) in the Lake Manyara region (2013-03-16; photo G. Quénéhervé).

isolated in time (Huxman & *alii*, 2004). Small rainfall pulses falling on dry soil surfaces wet only the uppermost part of the soil and a great amount of the soil moisture is accordingly lost by direct evaporation of the bare soil (Sala & Lauenroth, 1982). The soil evaporation front, deepening over time into the soil profile following the topsoil drying, is based on the solar energy reaching the soil surface as well as soil hydraulic properties and root densities (Wallace & *alii*, 1999; Schwinning & Sala, 2004). Rainfall on bare soils change the properties at the vicinity of the soil surface due to physical and chemical processes (Mualem & Assouline, 1996).

When overland flow in sparsely vegetated semiarid regions is generated, it occurs on stretched slopes as prevalent laminar sheetflow. When runoff concentrates further down the slope it becomes turbulent and promotes sediment detachment that leads to linear depressions called rills that are consequently deepened into gullies (Ritter & *alii*, 2011; Wainwright & Bracken, 2011). The runoff on dryland slopes may be highly discontinuous because of spatial and temporal variability in precipitation and in surface properties. The surface roughness significantly affects the pathways and rates of flow transfer. In general, runoff after small precipitation events can only be short distance runoff (Lauenroth & Bradford, 2006). The authors also stated that the common assumption for semiarid regions is that the runoff part of the water balance is close to zero, and hence it is often ignored. Jensen et al. (1990) reported that runoff depends on the characteristics of precipitation and can only be neglected for a particular type of soil, i.e. coarse textured (sand and loamy sand) and moderately coarse textured soils (sandy loams). However, at the event scale there can occur remarkable amounts of surface runoff on top of all kinds of soil texture types (Zema & *alii*, 2012) especially after dry periods, as also experienced by the authors. Figure 1 shows a surface runoff immediately after a 15 mm (in 40 min) event close to the Makuyuni village.

The rate at which water enters the soil is called infiltration rate or infiltration capacity, typically measured in mm/h. Most dryland soils are rarely saturated (Wainwright & Bracken, 2011), therefore the infiltration rate has normally a high initial value that decreases with time until it becomes fairly steady, called final infiltration rate. When rainfall exceeds the rate at which water can infiltrate the ground, surface runoff will be produced, accordingly called Hortonian overland flow (Bracken & Croke, 2007). Generally, as shown by various authors (Mualem, 1976; van Genuchten, 1980; Kutílek & Nielsen, 1994), infiltration rate (Q) is a function of soil water content (Θ) and soil water tension (Ψ). When water is applied into a dry soil, initially, most of the water is absorbed by the capillary potential of the soil matrix. The capillary force triggers the initial water infiltration process. Subsequently, as infiltration proceeds, the gravitational force becomes dominant (Philip, 1957). The critical matrix potential at which air enters the largest pores of a saturated soil is expressed as air entry value. As shown by Regner & *alii* (1999) infiltration processes consist of a soil matrix triggered micropore flow and a soil structure dependent macropore flow. In soils with dominant matrix driven processes, such as coherent soils, the infiltration from 0 tension up to the air entry value normally decreases. When macropores are present, water penetrates the soil mainly by these. The soils dominated by macropores show an immediate increase in infiltration when water tension is rising (Renger & *alii*, 1999; Schwärzel & Punzel, 2007). Apart of other factors like slacking, clogging, drop impact and air entrapment

that we do not consider in this study, infiltration and thus, surface runoff processes are strongly related to the soil's micro- and macropore distribution. Infiltration equation as stated of Philip (1975):

$$I = S \cdot t^{-\frac{1}{2}} \pm A \cdot t \qquad (1)$$

where I is infiltration rate; S is sorptivity; t is infiltration interval; and A is a constant, depending on water content (Θ) and soil water tension (Ψ).

The main objective of this study is to propose a simple approach to assess surface infiltration and runoff generation processes under semiarid climate conditions on hillslope scale. Especially we are interested in the infiltration rates and potential surface runoff at the end of the dry season. This goal is achieved using basic low budget, non-invasive methods that are easily applicable. We focus on the runoff generation mechanisms at hillslope scale with a characteristic soil catena for specific rainfall events. We do not tackle effects such as surface sealing, clogging or crusting since in the described conditions of semiarid environments a sophisticated measurement of these parameters is often not feasible. Instead, we concentrate on infiltration rates triggered by water content and water tension. The hypothesis is that, especially after the dry seasons soils have high water tensions and hence, the isolated rainfall events produce high amounts of surface runoff especially on fine-grained soils. Thus, water conduction is lower than in saturated conditions and consequently the overall infiltration rates quite low. Therefore, we performed detailed surface infiltration measurements using a tension infiltrometer and gained information about surface soil texture distribution. We monitored rainfall events over a three years period and estimated the evapotranspiration dynamics and land cover patterns and validated overland flow volumes with automatic surface runoff detectors.

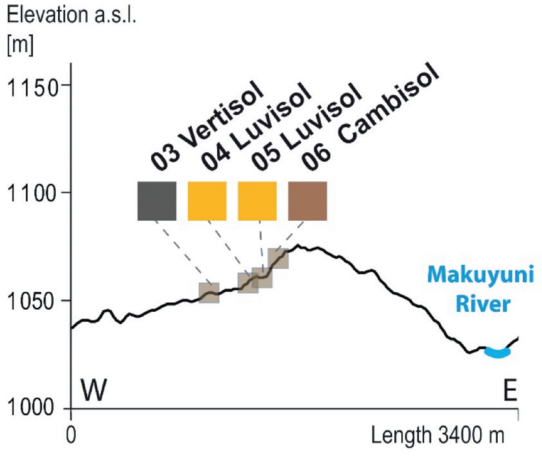

FIG. 2 - Soil transect with three different soil types according to World reference base for soil resources (FAO, 2014).

MATERIALS AND METHODS

STUDY AREA

The study area is located in Northern Tanzania in the eastern branch of the East African Rift System. It is drained by the Makuyuni River (catchment area ~3080 km²) which is flowing into the endorheic Lake Manyara. The prevailing savannah climate is characterized by bi-modal rainy seasons (Sep – Dec and Mar – May) with mean annual rainfall of ca. 500 mm and a strong inter-annual variability. The mean annual temperature is about 27°C, during short dry season (Jan – Feb) 30°C, during long rain season (Mar – May) 26°C, during long dry season (Jun – Sep) 22°C, and during short rain season (Oct – Dec) 27°C.

The study area has an extent of ca. 50 hectares and is located at the Manyara Ranch Conservancy. The morphology is characterized by a low angle stretched slope between 0 – 2.7° dipping towards north west (fig. 2). On the upper slopes Cambisols occur that are developed on tephra deposits and have therefore remaining andic properties (FAO, 2014). They also show leaching of carbonates towards the subsoil where $CaCO_3$ concretions are forming. On the midslope Rhodic Luvisols are located with loamy testure. The soil types in these localities are characterized by a high silica skeleton content with an average quartz mineral diameter of 1 cm. The Luvisol grade laterally into vertic horizons in lower landscape positions, the clay content is increasing and more active layer clays are accumulated. Thus, in the lower slope positions normally Vertisols are found.

FIELD DATA AND REMOTE SENSING ANALYSIS

To test the hypotheses, we conducted detailed surface infiltration measurements and gained information about surface soil texture distribution. Moreover, we monitored rainfall events over a three years period and estimated the evapotranspiration dynamics and landuse patterns. Overland flow volumes were assessed with automatic surface runoff detectors. The calculation of the runoff volumes were performed for single precipitation events. Moreover, we measured the relevant parameters (described below) in the field and in the laboratory or estimated these using remote sensing techniques as outlined below.

DGPS survey

We used a ProMark-3 differential GPS (DGPS) system in order to get very high-resolution digital topographic information. About 36,400 kinematic point measurements were measured and then post processed to orthometric heights (EGM96). The kinematic survey performance of the equipment is 0.012 m + 2.50 ppm (horizontal) and 0.015 m + 2.50 ppm (vertical) (ashtech, 2010). As the rover device was installed on a pole and variations occurred while it was carried over different landforms, we expect a vertical accuracy < 0.1 m + 2.50 ppm. Data acquisition took place in early March 2012, at the end of a short dry period. Thus vegetation and especially leaf cover was sparse and the sky

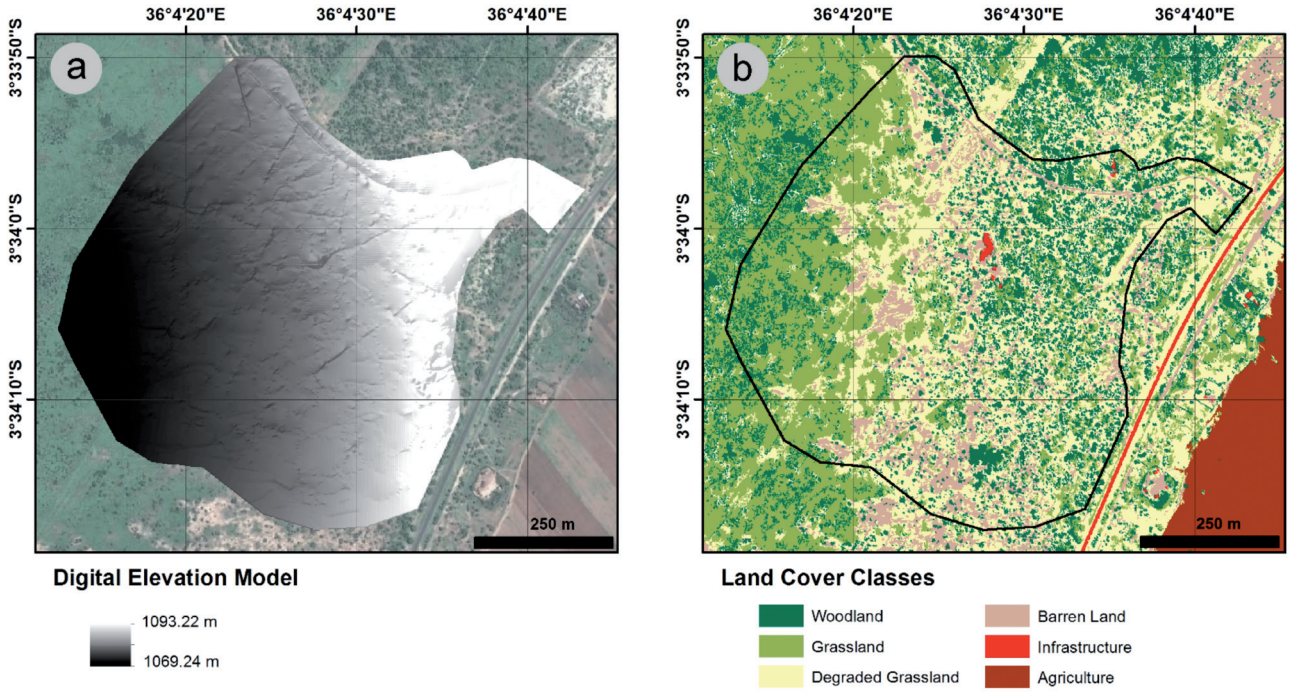

FIG. 3 - Surface runoff shortly after a precipitation event of 15 mm (in 40 min) in the Lake Manyara region (2013-03-16; photo G. Quénéhervé).

visibility of the GPS antenna and the resulting GPS signal lock was excellent. The sampling strategy was adapted to the constrained accessibility by bush vegetation.

The accuracy of the resulting digital elevation model (DEM) depends on the operational GPS precision, as well as the distribution and density of the GPS samples (Nico & *alii*, 2005). Visible drainage lines with a minimum depth of 5 cm were mapped separately with a kinematic survey and function as stream lines for the DEM building. The applied interpolation method is based on the ANUDEM algorithm, which allows the consideration of drainage enforcement to create a hydrological correct DEM (Hutchinson, 1989); Figure 3.

Land cover classification

For the derivation of land cover classes within the study area a multispectral WorldView-2 scene (acquired 2011-02-21; pan-sharpened to 0.5 m ground sampling distance) was utilized. For the analysis the three visible bands (RGB) as well as one near infrared band were available. Following an object based image analysis approach (Blaschke, 2010) five different land cover classes were distinguished (tab. 1) and validated in the field.

Soil characteristics

The calculation of the runoff volumes for single precipitation events is based on relevant parameters measured in the field and in the laboratory or estimated using remote sensing techniques. We measured soil texture for topsoil at 61 locations with a simple finger test method, according to USDA (1993). Additionally, we conducted laboratory analyses from four soil profile locations along a transect (fig. 1). Soil samples were air-dried and sieved (<2 mm). Texture was measured with the Bouyoucos Hydrometer Method after dispersing the samples with 1N Sodium hexametaphosphate and represented according to the United States Department of Agriculture classification (USDA, 1993). Organic Carbon was analysed using the Springer and Klee method (Springer & Klee, 1954). The field reference collection and the laboratory samples resulted into three soil classes, namely Cambisol, Luvisol, and Vertisol (tab. 2).

Meteorological parameters

Our study area is equipped with a multi-sensor climate station (Meteo combined with EnviLog MAXI data logger

TABLE 1 - Land cover classes

Class Number	Class Name	Description
1	Woodland	Trees and shrubs (> 1m)
2	Grassland	Grass, small bushes and sedges (permanent)
3	Degraded Grassland	Dry and sparse grassland (> 33% bare soil)
4	Barren Land	> 66% bare soil
5	Infrastructure	Buildings and paved roads

by EcoTech, Germany) that measures 6 parameters: wind speed and direction, precipitation, air temperature, relative humidity as well as air pressure. Data are measured with high temporal resolution of 10 min intervals and have been collected from March 2010 up to present.

Soil infiltration

With the hood infiltrometer (Umwelt-Geräte-Technik GmbH, Germany), which is a type of tension infiltrometer (Schwärzel & Punzel, 2007), water infiltrability is determined for the soil surface. The unsaturated conductivity was calculated following Wooding (1968) (Equation 2) and (Umwelt-Geräte-Technik, 2005) (Equation 3):

$$Q = \pi a^2 k_u \left(1 + \frac{4}{\pi \alpha a}\right) \quad (2)$$

$$\alpha = \frac{\ln\left(\frac{Q_1}{Q_2}\right)}{h1 - h2} \quad (3)$$

where Q is steady-state flow; a is radius of the infiltration area; k_u is hydraulic conductivity as a function of water tension; and h is water tension.

Accordingly, hydraulic conductivities for different tensions can be calculated using Equations 4 and 5, after Umwelt-Geräte-Technik (2005):

$$k(h_1) = \frac{\frac{Q_1}{\pi a^2}}{\left(1 + \frac{4}{\pi \alpha a}\right)} \quad (4)$$

$$k(h_2) = \frac{\frac{Q_2}{\pi a^2}}{\left(1 + \frac{4}{\pi \alpha a}\right)} \quad (5)$$

The capillary theory can be used to estimate the size of pores excluded from the transmission of infiltration at different pressure heads. Pore diameters can be predicted from Equation 6 (Sauer & Logsdon, 2002):

TABLE 2 - Soil Properties of the Soil Profiles[a].

Soil Depth	Particle size composition %			Class USDA	Corg (%)	Munsell soil colour
	Sand	Silt	Clay			
				03 Haplic Vertisol		
10 cm	42·3	36·8	20·9	L	0·77	5 YR 3/1
20 cm	35·0	28·7	36·3	CL	0·94	5 YR 2.5/1
30 cm	34·7	25·3	40·0	CL	1·23	7.5 YR 2.5/1
40 cm	35·1	24·2	40·7	C	1·03	5 YR 2.5/1
50 cm	31·2	27·3	41·5	C	0·93	7.5 YR 2.5/1
60 cm	31·1	24·5	44·4	C	1·05	7.5 YR 2.5/1
				04 Rhodic Luvisol		
10 cm	41·2	39·1	19·7	L	1·41	7.5 YR 4/3
20 cm	39·5	30·0	30·5	CL	1·27	7.5 YR 2.5/3
40 cm	37·7	26·0	36·3	CL	0·81	2.5 YR 2.5/2
				05 Rhodic Luvisol		
10 cm	54·3	34·1	11·6	SL	1·32	10 YR 3/4
20 cm	53·1	35·5	11·4	SL	0·95	7.5 YR 4/6
30 cm	51·4	36·4	12·2	L	0·90	5 YR 4/4
40 cm	51·5	37·3	11·2	L	0·65	5 YR 4/6
50 cm	47·3	37·0	15·8	L	0·72	5 YR 4/6
60 cm	46·0	37·2	16·8	L	0·64	7.5 YR 4/6
				06 Andic Cambisol		
10 cm	67·6	20·9	11·5	SL	20·5	7.5 YR 3/4
40 cm	57·7	24·2	18·1	SL	11·8	7.5 YR 4/6

[a]Soil classes after USDA (1993): L loam, CL clay loam, C clay, SL sandy loam; Soil colour under dry conditions after Munsell Soil Color Charts.

$$d = -\frac{4\,\sigma\,cos\alpha}{\rho\,g\,h} \quad (6)$$

where σ is the surface tension of water, N/m, assumed to be 0.072 at 25°C; α is the contact angle between water and pore wall, assumed = 0°, cos(0) = 1; ϱ is the density of water, kg/m³; and g is the gravitational acceleration, 9.8 m/s². Therefore, a higher suction or tension corresponds to an infiltration where the bigger pore sizes in the soil matrix are successively excluded from water transmission. The water tensions of -2 cm and -4 cm equal to pore sizes of 1.47 mm and 0.73 mm, respectively. In general, we assumed that soil pores are represented to be cylindrical, vertical tubes. Generally, the pressure 0 cm water column and two suctions have been measured at 40 locations.

Spatial modelling of soil hydrological characteristics

To get a spatially continuous data set of infiltration values and soil texture we utilized a stochastic modelling approach. In this study, a boosted regression tree approach (BRT) (Friedman, 2002) is applied using dependent and independent variables. BRTs employ a learning algorithm to identify a model that best fits the relationship between the predictor variables (an attribute set of, in this case, environmental variables) and the response variables, here the soil texture and infiltrability. The dependent variable is the soil texture measured for 61 locations within the study area, analysed with finger test (according to USDA (1993)). As independent variables the delineated landcover from multispectral WorldView-2 data as well as four terrain indices have been selected: (i) land cover classes, (ii) topographic wetness index (TWI) (after Beven & Kirkby, 1979), (iii) vertical distance to channel network, (iv) channel network base level (both after Olaya & Conrad, 2009), and (v) transport capacity (TCI) (Moore & *alii*, 1991). The indices ii to v are based on the derived hydrological correct DEM (see Moore & *alii*, 1993).

We utilized the TreeNet model (Salford Systems) also known as stochastic gradient boosting (Elith & Leathwick, 2009). The models' predictive performance is assessed by constructing the receiver operating characteristics (ROC) curves for each response variable, both for training and test data (Fielding & Bell, 1997). In a ROC curve the sensitivity is plotted over the false positive rate (1-Specificity) for all possible cut-off points (Swets, 1988). The quality of a ROC curve is quantified by the measurement of the parameter area under the ROC curve (AUC; Hanley & McNeil, 1982). The AUC is shown to be independent of prevalence (Manel & *alii*, 2001) and is considered a highly effective measure for the performance of ordinal score models. A perfect discrimination between positives and negatives has a ROC plot that passes through the upper left corner (100% sensitivity, 100% specificity), so that the AUC is equal to 1 (Reineking & Schröder, 2006). According to (Hosmer & *alii*, 2013) AUC values exceeding 0.7/0.8/0.9 indicate acceptable/excellent/outstanding predictions.

Automatic surface runoff detectors

Surface runoff was measured with automatic surface runoff detectors (SRD) that measure surface runoff height and duration. SRDs were distributed along the slope system to account for the runoff generation dynamics on different slope segments and thus, topographic positions. The SRD devices are placed on the surface whilst the logger unit is buried in the soil (fig. 4). When runoff height grows the electric contacts are closed sequentially transmitting a signal that is then reported to the logger storage unit. In this experimental setup, we placed logger units according to Figure 4b right side with equal spacing of contacts. The distances between the electric contacts are 5 mm, reaching up to 3 cm above ground. Hence, the device is able to measure a water column of 3cm and has a sensitivity of 5mm. The advantage of our study area and of semiarid environments in general is the sparse vegetation cover during dry periods, and hence the disturbance of runoff due to plants is minimized. Moreover, in most of the cases precipitation is moderate to low, so runoff is normally not accumulating deeper than the contact zone of the SRDs.

Runoff calculation

To calculate a simple water balance model, the relevant input parameters such as i) the precipitation input, ii) the evapotranspiration, iii) the infiltration rate, and iv) the resulting runoff hast to be measured (tab. 3).

The measured infiltration values are further attached to the regionalized model of the surface texture. This cre-

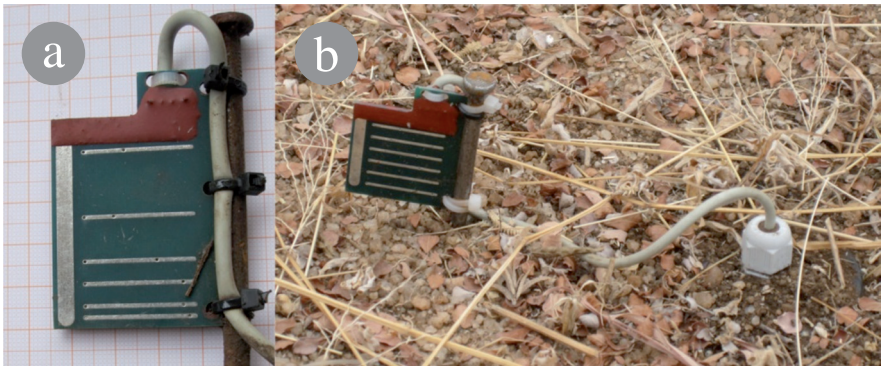

Fig. 4 - a) Close up of the sensor head of the Surface Runoff Detector. b) Installed device on the Manyara Ranch Conservancy test slope with the drainage coming from the right, shown with the blue arrow. (Photos: G. Quénéhervé).

TABLE 3 - Rainfall events, potential evapotranspiration, and calculated runoff characteristics.

Event number	Day of year	Rainfall duration [min]	Rainfall depth [mm]	Average rainfall intensity [mm/h]	PET_{Turc} [mm/ event][a]	Rainfall depth (P) - PET [mm]	Infiltration, tension $h0_2$ [mm]	Q_{h0} = P - PET - I [mm][b]	Infiltration, tension h2 [mm]	Qh_2 = P - PET - I [mm]	Infiltration, tension h2max [mm]	Q_{h2max} = P - PET - I [mm]
1	283	80	54.61	40.96	4.89	49.72	26.85	22.87	20.59	2.28	14.19	35.53
2	296	260	21.46	4.95	7.16	14.30		~		~		0.11
3	232 + 233	310	10.38	2.01	-	10.38		~		~		~
4	335	150	27.99	11.20	8.10	19.89		~		~		5.70
5	340	280	16.49	3.53	-	16.49		~		~		2.30

[a]PET: - indicates a night event, evapotranspiration is set to 0; bQ: ~ no runoff, all P is infiltrated into the soil column

ates a raster model with infiltration values as attributes. A single-cell raster based water balances model (Equation 7) was then utilized for a weighted flow algorithm based on a deterministic infinity flow approach following (Tarboton, 1997), the GIS modelling was done with SAGA GIS (Conrad, 2006). For the sake of simplicity the runoff calculation do not take into account surface roughness parameters.

$$R = P–I \quad (7)$$

where R is water balance and P is precipitation.

RESULTS

PRECIPITATION ANALYSIS

For this study we focus on the period October to December 2010, where 5 rainfall events occurred, which produced substantial runoff that was captured by the surface runoff detectors. Table 4 shows the mean daily meteorological data for each day of the recorded events and Table 5 the soil hydraulic conditions.

DGPS AND REMOTE SENSING DATA PROCESSING

For the evaluation of DGPS measurements, a regular 1 m point grid was computed for the study area (ca. 440,000 points). For each point of the produced digital elevation model (the centroid of the 1 x 1 m grid) the distance to the closest DGPS measurement was calculated. The average distance to a reference point is 5.43 m with a standard deviation of 4.7 m and a maximum distance of 32.65 m. 48.8% of all interpolated points are within a maximum distance of 4 m to a DGPS measurement point, whereas only 1.2 % within a distance greater than 20 m.

Including spectral and textural attributes, we discriminated five land cover classes with an overall accuracy of 88.98% (Kappa 0.86), validated with ground reference information. In contrast to the land use class “Grassland” the

TABLE 4 - Mean daily climatic dataa for the recorded events in 2010.

Day of year	Tmax [°C]	Tmin [°C]	mean T [°C]	mean RH [%]	meanhPa	PETTurc [mm/d]
283	34.0	17.6	24.8	37.65	893.01	219.89
296	29.6	18.6	23.2	38.74	892.39	198.35
232	31.2	18.6	23.4	43.99	892.73	187.64
233	32.6	18.7	24.7	44.64	891.90	199.9
335	32.1	18.1	23.4	41.23	890.98	194.47
340	31.9	19.6	23.1	42.87	889.74	186.72

[a]T temperature; RH relative humidity; hPa hectopascal; PET potential evapotranspiration

Table 5 - Measured tensions and according infiltration rates with hood infiltrometer.

Mess_ID	Tension h0	Infiltration h0 [mm/h]	Tension h1	Infiltration h1 [mm/h]	Tension h2	Infiltration h2 [mm/h]	Air entrytension
1	0	20.52	-2.0	13.99	none	none	-5.8
2	0	29.23	-3.4	21.14	-5.5	16.79	-9.5
4	0	14.93	-2.5	11.82	none	none	-7.1
5	0	34.83	-3.0	33.58	none	none	-5.2
8	0	31.00	-1.2	30.87	-3.1	29.63	-15.1
10	0	19.28	-4.0	13.68	-8.0	9.33	-15.1
11	0	15.55	-4.0	9.33	-9.0	7.46	-22.0
13	0	32.34	-1.5	26.12	-2.4	19.90	-7.8
14	0	21.77	-3.4	18.66	none	none	-7.1
15	0	84.58	-4.0	31.72	none	none	-6.9
16	0	32.96	-4.0	25.50	-8.0	19.90	-10.7
17	0	24.25	-3.5	20.52	-6.0	15.55	-12.4
19	0	38.56	-2.7	29.85	-2.8	29.02	-7.5
20	0	43.53	-4.0	18.35	-6.0	13.68	-9.3
22	0	13.33	-2.5	8.71	-4.8	6.66	-8.5
23	0	26.65	none	none	none	none	-11.0
23	0	36.07	none	none	none	none	-11.0
24	0	14.66	-6.3	9.95	-9.2	2.69	-13.0
25	0	14.61	-4.0	7.00	-7.5	4.35	-8.8
26	0	114.01	-4.0	62.19	-7.2	38.35	-8.6
27	0	74.63	-3.0	43.53	-5.1	33.17	-18.0
28	0	202.11	-3.9	128.26	-7.0	90.17	-9.5
29	0	15.55	-4.4	9.33	-9.5	7.46	-13.1
30	0	18.66	-4.4	11.19	-7.0	5.60	-7.6
31	0	32.34	-6.0	34.83	-12.0	23.01	-17.4
32	0	33.58	-3.0	22.39	-5.4	18.66	-9.6
33	0	97.95	-4.0	60.63	-5.5	23.63	-7.6
34	0	69.44	-2.2	49.13	-4.6	42.91	-9.7
35	0	98.46	-4.0	66.85	-6.0	65.30	-9.0
36	0	31.09	-4.4	18.66	none	none	-7.5
37	0	71.52	-1.4	59.08	-2.2	49.13	-3.0
38	0	39.18	-3.5	32.34	-7.0	26.85	-13.3
39	0	18.66	-4.4	15.55	-6.7	12.83	-8.7
40	0	11.11	-4.6	7.15	none	none	-14.1
41	0	37.31	-2.0	41.04	-5.0	31.72	-10.3
42	0	55.19	-3.0	23.32	-6.1	13.33	-9.1
43	0	15.55	-4.4	9.33	-8.8	6.53	-13.8
44	0	37.31	-2.7	20.52	-5.3	13.60	-8.6
45	0	29.85	-3.2	24.88	-7.1	16.17	-7.7

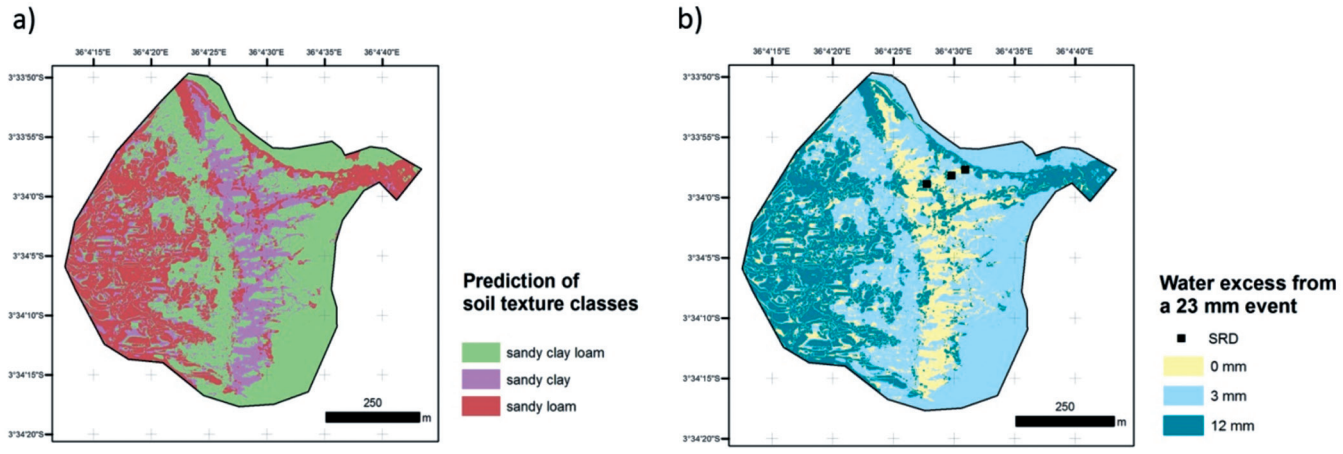

FIG. 5 - a) Prediction of soil texture classes (USDA taxonomy) according to the boosted regression tree based classification model. b) Spatial distribution of water excess calculated for a precipitation event of 23 mm (~event number 1), based on the predicted soil texture class.

classes "Degraded Grassland" and "Barren Land" show a high percentage of bare soil. The later ones are highly affected by dry and wet seasons concerning their vegetation share and are in result highly affected by overgrazing and erosional processes. The highest confusion between the classes turned out to occur between "Grassland" and "Degraded Grassland" (fig. 3b).

REGIONALIZATION OF SOIL SURFACE TEXTURE

All DEM-based independent variables show a high contribution to the best fitted classification tree model. Only the land cover classification is found to be of no significance to soil texture distribution. The modelling based on the remaining four terrain indices shows a very good model performance. The modelled classes 'sandy loam' and 'sandy clay loam' with an AUC value of more than 0.8 show an excellent prediction output. The class 'sandy clay' with an AUC value of 0.93 indicates to have an outstanding prediction performance.

The according regionalization based on the TreeNet model is shown in Figure 5a. The results show a sequence of textures from sandy clay loam on the eroded cambisols in the upper slope positions to sandy clay textures at mid slope positions. Toe slopes are characterized by sandy loam textures and vertic features. In Figure 6 the relation of texture and infiltration is shown for the 0 tension measurements in boxplots a) to d). As expected there is a close relation between texture and infiltration rates at 0 tension. The higher tensions h_2 are measured in relation to the specific air entry value of the soil's matric potential see boxplots e) to h). Figure 7 shows the relation between texture and reached tensions. As expected the highest tensions are measured in the soils with highest clay content and they are lowest in the soils with dominant sand fractions. The median tension infiltration value of the respective textures classes were then attributed to the soil texture map for the runoff modelling.

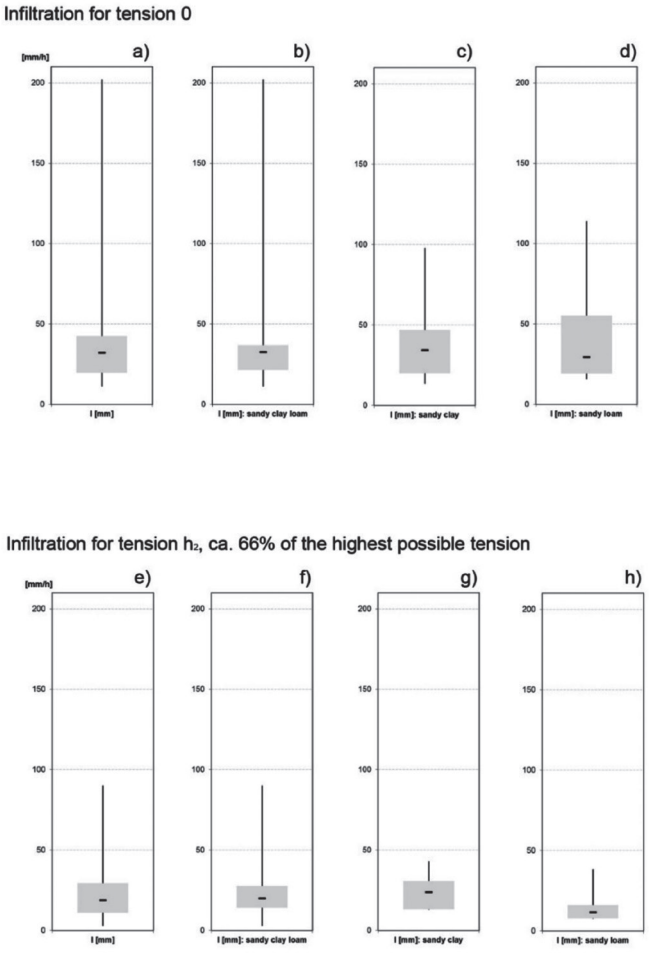

FIG. 6 - Infiltration rate (I) of 0 tension, in mm/h, for all locations a), and for the different soil texture classes b) – d). Accordingly infiltration rate of tension h2 for all locations e), and for the different soil texture classes f) – h).

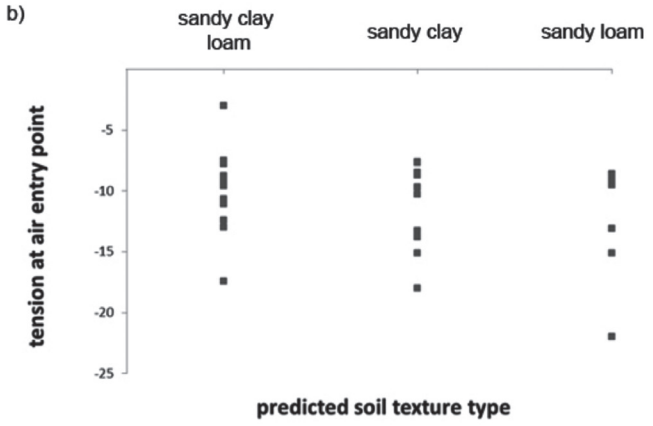

FIG. 7 - The relation between predicted soil texture class and reached tensions, in a) the tensions measured at h2, and in b) tensions at air entry value.

WATER BALANCE MODELLING

The water balance was calculated after Equation 7 for the test area on a 1m x 1m pixel basis. The calculation was performed for the surface infiltration at 0 tension and highest measured tensions (h_2). Figure 5b shows the spatial distribution of the infiltration excess for the highest measured tension. Sandy loam soils (in dark blue) show a fast response to surface sealing due to their texture partitioning. They are therefore prone to a fast surface runoff development. The Luvisols (sandy loam and loam fraction) show a high water flux and only small runoff is calculated (in light blue) or even none (yellow). Within the soil column, the picture will be the other way round, with a high micropore flux (Luvisols) lower infiltration values at higher tension values are expected, whereas soils with macropores (Vertisols) show a higher infiltration. The water balances were subsequently utilized as weighting surface in a weighted flow accumulation algorithm. This model is based on the Multiple Flow Direction algorithm (after Seibert & McGlynn, 2007) and counts the number of cells draining into a given cell. Figure 8 shows the produced runoff volumes for the infiltration scenario shown in Figure 5b.

SURFACE RUNOFF MEASUREMENT VIA SRD

For each of the 5 rainfall events (>5 mm rainfall within 1 hour) occurring from October to December 2010, we compared the data to the recorded discharge height in the SRDs. All 5 events have been recorded in each of the available SRDs. Generally, the SRDs characterize the actual surface-runoff amounts on hillslope scale in a very high temporal resolution (5 min intervals). Consequently, SRDs can be used to roughly validate water balance calculations and related runoff processes. For the single SRD locations we estimated the upslope contributing area with SAGA-GIS software using a deterministic infinity flow direction algorithm following Tarboton (1997). Measured values of surface runoff are shown in Table 6.

DISCUSSION

In this study we focus on the spatial distribution of infiltration rates. As shown, infiltration in semiarid savannah dry lands of northern Tanzania is mainly depending on spe-

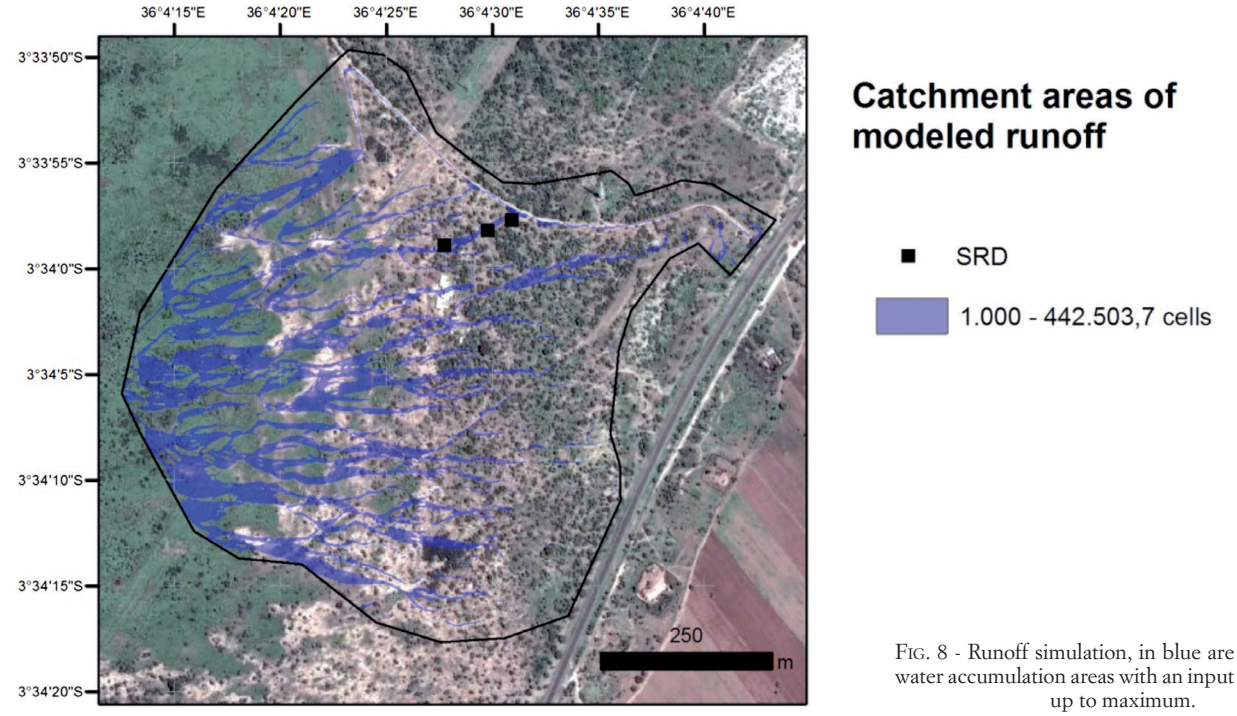

FIG. 8 - Runoff simulation, in blue are depicted the water accumulation areas with an input of 1.000 cells up to maximum.

TABLE 6 - Measured discharge from surface runoff detectors..

ID	Catchment area [m²]	Rainfall event	runoff [mm]	RI [mm/h]	Rainfall event	runoff [mm]	RI [mm/h]	Rainfall event	runoff [mm]	RI [mm/h]	Rainfall event	runoff [mm]	RI [mm/h]	Rainfall event	runoff [mm]	RI [mm/h]
A	278.62	1	107.5	1.34	2	117.5	1.47	3	25	0.31	4	203	2.54	5	108.5	1.36
B	608.08		22	0.28		240	3.00		85	1.06		321.5	4.02		171	2.14
C	569.68		202.5	2.53		300	3.75		95	1.19		298.5	3.73		162	2.03

[a]RI: average runoff intensity

cific soil physical characteristics and climatic conditions. The carbonatic volcanic ash and tuff/tephra deposits of the Makuyuni area are characterized by Andic Cambisols and Rhodic Luvisols with low activity clays developed on the upper slopes and flat summit areas. These soils show an intensive carbonate leaching (decalcification) and accumulation of carbonates (concretions) in the deeper subsoil or further downslope. On the slope ridges the soils are often eroded. The material is washed along the surface and deposition dominates in the toe slope situations. The structure of the soils is changing from matrix dominated soils on the slope ridges and mid-slope positions, towards vertic soils showing a distinct secondary macropore structures due to active layer clays (typically consisting of smectite and illite clays). The soil catena itself documents the intense sediment transport with surface runoff. Infiltration at different textures vary significantly. Especially in micropore dominated soils the infiltration is mainly triggered by the tension values or in other words is triggered by different humidity conditions of the uppermost soil horizon before rainfall starts. Generally, infiltration is decreasing for highest measured tensions by 18.74 %. For the sake of simplicity, we kept the evapotranspiration constant and do not consider soil water storage to calculate the water balance and hence, overland flow generation.

The GIS-based simulation of runoff depending on pixel water balances shows that for a detailed hillslope scale analysis a high-resolution digital elevation model is crucial. This is because all further analyses such as topographic indices, e.g. runoff direction and accumulation, are based on the accuracy of the height estimations. Particularly, the creation of a hydrological correct DEM is essential for further hydrological modeling. Therefore, sophisticated statistical methods provide accurate spatial pattern of soil surface texture. Finally, we calculated the different runoff volumes in mm/h and, make them comparable, converting also the rainfall events to average rainfall intensity in mm/h. We show that for 0 tension only the highest event of 40.6 mm/h (rainfall intensity) produced runoff whereas all other events do not show surface runoff. If tension increase the runoff is getting higher for the highest rainfall event (event 1) but still no runoff is produced for the other events (events 2-5). Only when the highest measured tension is utilized the runoff even for the other events can be modelled as shown in Table 3.

For all events runoff is produced and detected in the distributed SRDs. This means that the infiltration values for 0 and h_2 tension used in the modelling are too high for the events 2-5. Only if we use the highest tension (h_{2max}) realistic surface runoff values are simulated. This means that the contributing area for the three SRDs is mainly characterized by homogeneous soils dominated by matrix pore triggered infiltration with small pore sized at sandy loam textures. Tension for this texture (sandy loam) can reach very high suctions characterized by a high air entry value. Hence, the measured highest tensions may be even higher if the measurement is performed close to the air entry point. Consequently, the infiltration becomes even lower.

CONCLUSIONS

The study presents a simple low budget approach to assess soil infiltration and surface runoff values. We show that infiltration processes in semiarid dryland conditions are mainly depending on the soil physical characteristics such as soil water tension and the moisture conditions of the topsoil before the precipitation event starts. Saturated conductivities often used to calculate the surface runoff yield too high infiltration values to explain observed surface runoff. In this study we measured the shallow laminar runoff at the surface using SRDs. Moreover, infiltrations were measured at different tensions simulating various soil humidity conditions. We illustrated with a simple water balance approach, that infiltrations measured at 0 tension produce too high infiltration values in order to generate surface runoff. Especially in micropore dominated homogeneous soils water tension triggered infiltration rates play a crucial role. Thus, on the slope system studied in this investigation surface runoff was only produced if the highest tension infiltration rates were used corresponding to "drier" soil conditions. Consequently, it is very important what kind of soil types are present in a catchment and to what kind of infiltration scheme they are belonging to. Especially in homogeneous soils with low activity clays notable surface runoff can be produced if the soil is very dry when precipitation starts. This example from a hillslope scale water balance model demonstrates the importance of integrated field work measurements (especially the incorporation of surface runoff detectors) and computer-based simulations in hydrological research.

The automatic surface runoff detectors offer a helpful insights into actual overland flow dynamics and, especially, for the quantification of those. This approach can provide useful additional information on water balance modelling. Primarily the verification of single parameters of the water balance equation can further be validated and evaluated.

References

ASHTECH (2010) - *ProMark 3 RTK.* http://www.spectraprecision.com/products/gnss-surveying/promark3-rtk-2655.kjsp, Nov 4, 2014.

Beven K.J. & Kirkby M.J. (1979) - *A physically based, variable contributing area model of basin hydrology.* Bulletin of the International Association of Scientific Hydrology, 24, 43-69.

Blaschke T. (2010) - *Object based image analysis for remote sensing.* ISPRS Journal of Photogrammetry and Remote Sensing, 65, 2-16.

Borselli L., Torri D., Poesen J. & Sanchis P.S. (2001) - *Effects of water quality on infiltration, runoff and interrill erosion processes during simulated rainfall.* Earth Surface Processes and Landforms, 26, 329-342.

Bracken L.J. & Croke J. (2007) - *The concept of hydrological connectivity and its contribution to understanding runoff-dominated geomorphic systems.* Hydrological Processes, 21, 1749–1763.

Conrad O. (2006) - *SAGA - Program structure and current state of implementation*. In: Böhner, J. & MacCloy, K.R. (Eds.) SAGA-analysis and modelling applications. Goltze, Göttingen, 39-52.

Critchley W. & Siegert K. (1991) - *Water Harvesting. A Manual for the Design and Construction of Water Harvesting Schemes for Plant Production,* Rome, Italy, 157 pp.

Elith J. & Leathwick J.R. (2009) - *Species Distribution Models: Ecological Explanation and Prediction Across Space and Time.* Annual Review of Ecology, Evolution, and Systematics, 40, 677-697.

FAO (2014) - *World reference base for soil resources. International soil classification system for naming soils and creating legends for soil maps*. FAO, Natural Resources Management and Environment Department.

Fielding A.H. & Bell J.F. (1997) - *A review of methods for the assessment of prediction errors in conservation presence/absence models.* Environmental Conservation, 24, 38-49.

Friedman J.H. (2002) - *Stochastic gradient boosting. Nonlinear Methods and Data Mining.* Computational Statistics & Data Analysis, 38, 367-378.

Hanley J.A. & McNeil B.J. (1982) - *The meaning and use of the area under a receiver operating characteristic (ROC) curve.* Radiology, 143, 29-36.

Hosmer D.W., Lemeshow S. & Sturdivant R.X. (2013) - *Applied logistic regression,* 3rd ed. Wiley, Hoboken N.J., 1 online resource (xvi, 500 pp.)

Hutchinson M.F. (1989) - *A new procedure for gridding elevation and stream line data with automatic removal of spurious pits.* Journal of Hydrology, 106, 211-232.

Huxman T.E., Snyder K.A., Tissue D., Leffler A.J., Ogle K., Pockman W.T., Sandquist D.R., Potts D.L. & Schwinning S. (2004) – *Precipitation pulses and carbon fluxes in semiarid and arid ecosystems.* Oecologia, 141, 254-268.

Jensen M.E. & Burman R.D. & Allen R.G. (1990) - *Evapotranspiration and irrigation water requirements. A manual.* American Society of Civil Engineers, New York, N.Y., xxviii, 332 pp.

Kutílek M. & Nielsen D.R. (1994) - *Soil hydrology.* Catena Verlag, Cremlingen-Destedt, 370 S. pp.

Lauenroth W.K. & Bradford J.B. (2006) - *Ecohydrology and the Partitioning AET Between Transpiration and Evaporation in a Semiarid Steppe.* Ecosystems, 9, 756-767.

Manel S., Williams H.C. & Ormerod S.J. (2001) - *Evaluating presence–absence models in ecology: the need to account for prevalence.* Journal of Applied Ecology, 38, 921-931.

Moore I.D., Gessler P.E., Nielsen G.A. & Peterson G.A. (1993) - *Soil Attribute Prediction using Terrain Analysis.* Transactions of the American Society of Agricultural Engineers, 57, 443-452.

Moore I.D., Grayson R.B. & Ladson A.R. (1991) - *Digital terrain modelling. A review of hydrological, geomorphological, and biological applications.* Hydrological Processes, 5, 3-30.

Mualem Y. (1976) - *A new model for predicting the hydraulic conductivity of unsaturated porous media.* Water Resources Research, 12, 513-522.

Mualem Y. & Assouline, S. (1996) - *Soil Sealing, Infiltration and Runoff*. In: Issar A. & Resnick S. (Eds.) Runoff, Infiltration and Subsurface Flow of Water in Arid and Semi-Arid Regions. Springer Netherlands, 131-181.

Nico G., Rutigliano P., Benedetto C. & Vespe F. (2005) - *Terrain modelling by kinematical GPS survey.* Natural Hazards and Earth System Science, 5, 293-299.

Olaya V. & Conrad C. (2009) - *Geomorphometry in SAGA*. In: Hengl, T. & Reuter HI (Eds.) Geomorphometry. Concepts, Software, Applications. Elsevier, Amsterdam, 293-308.

Philip J.R. (1957) - *The Theory of Infiltration: 1. The Infiltration Equation and its solution.* Soil Science, 83, 345-358.

Philip J.R. (1975) - *Stability Analysis of Infiltration.* Soil Science Society of America Journal, 39, 1042-1049.

Reineking B. & Schröder B. (2006) - *Constrain to perform: Regularization of habitat models.* Ecological Modelling, 193, 675-690.

Renger M., Stoffregen H., Klocke J., Facklam M., Wessolek G., Roth C.H. & Plagge, R. (1999) - *Ein autoregressives Verfahren zur Bestimmung der gesättigten und ungesättigten hydraulischen Leitfähigkeit.* Journal of Plant Nutrition and Soil Science, 162, 123-130.

Ritter D.F., Kochel R.C. & Miller J.R. (2011) - *Process Geomorphology,* 5. Ed. Waveland Press, Long Grove, Ill., 652 pp.

Sala O.E. & Lauenroth W.K. (1982) - *Small rainfall events: An ecological role in semiarid regions.* Oecologia, 53, 301-304.

Sauer T.J. & Logsdon S.D. (2002) - *Hydraulic and Physical Properties of Stony Soils in a Small Watershed. Soil Science Society of America Journal*, 66, 1947–1956.

Schwärzel K. & Punzel J. (2007) - *Hood Infiltrometer A New Type of Tension Infiltrometer.* Soil Science Society of America Journal, 71, 1438-1447.

Schwinning S. & Sala O. (2004) - *Hierarchy of responses to resource pulses in arid and semi-arid ecosystems.* Oecologia, 141, 211-220.

Seibert J. & McGlynn B.L. (2007) - *A new triangular multiple flow direction algorithm for computing upslope areas from gridded digital elevation models.* Water Resources Research, 43, W04501.

Springer U. & Klee J. (1954) - *Prüfung der Leistungsfähigkeit von einigen wichtigeren Verfahren zur Bestimmung des Kohlenstoffs mittels Chromschwefelsäure sowie Vorschlag einer neuen Schnellmethode.* Zeitschrift für Pflanzenernährung, Düngung, Bodenkunde, 64, 1-26.

Swets J.A. (1988) - *Measuring the accuracy of diagnostic systems.* Science, 240, 1285-1293.

Tarboton D.G. (1997) - *A new method for the determination of flow directions and upslope areas in grid digital elevation models.* Water Resources Research, 33, 309-319.

Umwelt-Geräte-Technik, 2005 - *Operating instructions for Hood Infiltrometer.* http://www.ictinternational.com.au/ugt/brochures/hood-infiltrometer.pdf, Nov 4, 2014.

USDA (1993) - *Soil survey manual. United States Department of Agriculture (USDA). Soil Survey Division, Washington, D.C.,* 437 pp.

van Genuchten, M.T. (1980) - *A Closed-form Equation for Predicting the Hydraulic Conductivity of Unsaturated Soils1.* Soil Sci. Soc. Am. J., 44, 892-898.

Wainwright J. & Bracken L.J. (2011) - *Runoff generation, overland flow and erosion on hillslopes*. In: Thomas, D. (Ed.) Arid Zone Geomorphology. Process, Form and Change in Drylands. Wiley-Blackwell, Oxford, 237-267.

Wallace J.S., Jackson N.A. & Ong C.K. (1999) - *Modelling soil evaporation in an agroforestry system in Kenya.* Agricultural and Forest Meteorology, 94, 189-202.

Wooding R.A. (1968) - *Steady Infiltration from a Shallow Circular Pond.* Water Resources Research, 4, 1259-1273.

Zema A.D., Bombino G., Denisi P., Licciardello F. & Zimbone S.M. (2012) - *Prediction of Surface Runoff and Soil Erosion at Watershed Scale: Analysis of the AnnAGNPS Model in Different Environmental Conditions*. In: Godone D. (Ed.), Research on Soil Erosion. InTech, 3-31.

(ms received 15 December 2014; accepted 15 May 2015)